J|A|C|S ARTICLES

Published on Web 11/06/2009

Multiplexed Imaging of Therapeutic Cells with Multispectrally Encoded Magnetofluorescent Nanocomposite Emulsions

Yong Taik Lim,[†] Young-Woock Noh,[†] Jee-Hyun Cho,[‡] Jung Hyun Han,[†] Bang Sil Choi,[†] Jina Kwon,[†] Kwan Soo Hong,[‡] Anisha Gokarna,[§] Yong-Hoon Cho,[§] and Bong Hyun Chung*,[†]

BioNanotechnology Research Center, Korea Research Institute of Bioscience and Biotechnology, Daejeon 305-806, South Korea, MRI Team, Korea Basic Science Institute, Ochang, Chungbuk, South Korea, and Department of Physics, Korea Advanced Institute of Science and Technology, South Korea

Received June 6, 2009; E-mail: chungbh@kribb.re.kr

Abstract: Here, we describe the fabrication of multispectrally encoded nanoprobes, perfluorocarbon (PFC)/quantum dots (QDs) nanocomposite emulsions, which could provide both multispectral MR and multicolor optical imaging modalities. Our strategy exploited the combination of the multispectral MR properties of four different PFC materials and the multicolor emission properties of three different colored CdSe/ZnS QDs. The PFC/QDs nanocomposite emulsions were fabricated by exchanging hydrophobic ligands coated onto CdSe/ZnS QDs using 1*H*,1*H*,2*H*,2*H*-perfluorooctanethiol, which renders the QDs to be dispersible in the PFC liquids. To provide biocompatibility, the PFC liquids containing QDs were emulsified into aqueous solutions with the aid of phospholipids. The distinct ^{19}F-based MR images of PFC/QDs nanocomposite emulsions were obtained by selective excitation of the nanocomposite emulsions with magnetic resonance frequency of each PFC, while a specific fluorescence image of them could be selected using appropriate optical filters. The uptake of PFC/QDs nanocomposite emulsions was high in phagocytic cells such as macrophages (90.55%) and dendritic cells (85.34%), while it was low in nonphagocytic T cells (33%). We have also shown that the nanocomposite emulsions were successfully applied to differentially visualize immunotherapeutic cells (macrophages, dendritic cells, and T cells) in vivo. The PFC/QDs nanocomposite emulsions are expected to be a promising multimodality nanoprobe for the multiplexed detection and imaging of therapeutic cells both in vitro and in vivo.

Introduction

Recent advances in the design and fabrication of nanostructured materials have been providing potential applications in biomedical areas ranging from disease diagnosis to therapy.[1−7] With the development of various contrast-enhancing nanoprobes, magnetic resonance imaging (MRI) has become one of the main molecular imaging technologies for disease diagnosis and monitoring the movement of cells.[8−13] The optical imaging that uses colored metallic nanoparticles, multispectral semiconductor quantum dots, or organic fluorophores has high sensitivity and multiplexing capabilities for in vitro detection and cell labeling.[14−18] In contrast, MRI's main advantage is its sensitivity through deep tissues that cannot be achieved by optical imaging. Thus, the dual-functional imaging nanoprobes to integrate the advantages of MR with the optical imaging capabilities are becoming increasingly important as molecular imaging contrast agents.[1−5] Nevertheless, none of these bimodal imaging nanoprobes based on ^{1}H-based MRI contrast agent is capable of distinguishing multiple targets simultaneously in vivo. Although the optical imaging nanoprobes have been widely exploited in biotechnology and biomedical research fields due to their

[†] Korea Research Institute of Bioscience and Biotechnology.
[‡] Korea Basic Science Institute.
[§] Korea Advanced Institute of Science and Technology.

(1) Wang, S.; Jarrett, B. R.; Kauzlarich, S. M.; Louie, A. Y. *J. Am. Chem. Soc.* **2007**, *129*, 3848–3856.
(2) (a) Park, J.-H.; Von Maltzahn, G.; Ruoslahti, E.; Bhatia, S. N.; Sailor, M. J. *Angew. Chem., Int. Ed.* **2008**, *47*, 7284–7288. (b) Beaune, G.; Dubertret, B.; Clement, O.; Vayssettes, C.; Cabuil, V.; Menager, C. *Angew. Chem., Int. Ed.* **2007**, *46*, 5421–5424.
(3) (a) Prinzen, L.; Miserus, R.-J. J. H. M.; Dirksen, A.; Hackeng, T. M.; Deckers, N.; Bitsch, N. J.; Megens, R. T. A.; Douma, K.; Heemskerk, J. W.; Kooi, M. E.; Frederik, P. M.; Slaaf, D. W.; van Zandvoort, M. A. M. J.; Reutelingsperger, C. P. M. *Nano Lett.* **2007**, *7*, 93–100. (b) Jin, T.; Yoshioka, Y.; Fujii, F.; Komai, Y.; Seki, J.; Seiyama, A. *Chem. Commun.* **2008**, *44*, 5764–5766. (c) Selvan, S. T.; Patra, P. K.; Ang, C. Y.; Ying, J. Y. *Angew. Chem., Int. Ed.* **2007**, *46*, 2448–2452. (d) Yi, D. K.; Selvan, S. T.; Lee, S. S.; Papaefthymiou, G. C.; Kundaliya, D.; Ying, J. Y. *J. Am. Chem. Soc.* **2005**, *127*, 4990–4991.
(4) (a) Santra, S.; Yang, H.; Holloway, P. H.; Stanley, J. T.; Mericle, R. A. *J. Am. Chem. Soc.* **2005**, *127*, 1656–1657. (b) Yang, H.; Santra, S.; Walter, G. A.; Holloway, P. H. *Adv. Mater.* **2006**, *18*, 2890–2894. (c) Tan, W. B.; Zhang, Y. *Adv. Mater.* **2005**, *17*, 2375–2380.
(5) (a) Mulder, W. J. M.; Koole, R.; Brandwijk, R. J.; Storm, G.; Chin, P. T. K.; Strijkers, G. J.; de Mello Donega, C.; Nicolay, K.; Griffioen, A. W. *Nano Lett.* **2006**, *6*, 1–6. (b) Koole, R.; Van Schooneveld, M. M.; Hilhost, J.; Castermans, K.; Cormode, D. P.; Strijkers, G. J.; Donega, C. D. M.; Vanmaekelbergh, D.; Griffioen, A. W.; Nicolay, K.; Fayad, Z. A.; Meijerink, A.; Mulder, W. J. M. *Bioconjugate Chem.* **2008**, *19*, 2471–2479.
(6) Frangioni, J. V.; Hajjar, R. J. *Circulation* **2004**, *110*, 3378–3383.
(7) Park, J. H.; Lee, S.; Kim, J.-H.; Park, K.; Kim, K.; Kwon, I. C. *Prog. Polym. Sci.* **2008**, *33*, 113–137.
(8) Yan, G. P.; Robinson, L.; Hogg, P. *Radiography* **2007**, *13*, e5−e19.
(9) Lorusso, V.; Pascolo, L.; Fernetti, C.; Anelli, P. L.; Uggeri, F.; Tiribelli, C. *Curr. Pharm. Des.* **2005**, *11*, 4079–4098.

sensitive and multiplexed detection capabilities at a cellular level, the low light penetration capability through a biological tissue (such as opaque animal or human) hampers the use of optical-based labels for noninvasive in vivo molecular imaging applications. Therefore, the development of multispectral MRI nanoprobes that can distinguish different types of cells in vivo is highly required for the in vivo multiplexed detection and molecular imaging in cell-based therapies.

In this study, we describe the fabrication of a novel-type bimodal imaging nanoprobe, PFC/QDs nanocomposite emulsions, which could provide both multispectral MR and multicolor optical imaging modalities. We have also shown that the multiple-detection capabilities of PFC/QDs nanocomposite emulsions could be successfully applied to visualize T cells, dendritic cells, and macrophages in vivo. Our strategy exploited the combination of the multispectral MR properties of ^{19}F-based molecules and the multicolor emission properties of fluorescent QDs. In this context, ^{19}F has excellent properties for MR detection and imaging in the sense that the background concentration of fluorine is essentially undetectable. In addition, the dynamic range and sensitivity of the chemical shifts from the specific local environments are much higher for fluorine than for hydrogen.[19−22] Hence, the highly distinguishing property of fluorine (^{19}F)-based MR spectroscopy and imaging could enhance the possibility of differentiating distinct ^{19}F signals from other element/compound in multispectral MR detections.[21,22] Thus, the selective excitation at specific resonance frequencies for each fluorine-based material could differentiate individual PFC-type-dependent MR signals. For the integration of optical imaging modalities with the excellent properties of ^{19}F-based PFC materials in MR detection, the colloidal QDs were exploited. Because of their nanometer-sized dimensions and unique optical properties for the simultaneous emission at various wavelengths with a single excitation source, QDs are currently being investigated for their applications as fluorescent biological probes and optical contrast agents in biomedical imaging.[23−27]

Results and Discussion

Scheme 1 shows a schematic illustration for the fabrication of the engineered PFC/QDs nanocomposite emulsions comprising of PFC liquids containing fluorescent QDs and phospholipids. Multispectral MR signals were distinguishable by using different types of PFC materials with distinct MR spectra. As QDs emissions are tunable for their sizes and chemical compositions, the multicolor QDs with minimum spectral overlaps could be incorporated into the PFC materials for wavelength tuning. To increase the compatibility of hydrophobic QDs with PFC, which have both hydrophobic and lipophobic properties, the coated QDs with hydrophobic ligands were exchanged with 1*H*,1*H*,2*H*,2*H*-perfluorooctanethiol. Three different colored QDs were then dispersed into four different PFC materials to have distinguishable ^{19}F-based MR spectra. Finally, the PFC liquids containing QDs were emulsified into aqueous solutions using phospholipids and high shear force.

We selected four different PFC materials for use as ^{19}F-based multispectral MR imaging nanoprobes. They were investigated for their independent detection using the specific spectrum of each PFC. The distinct magnetic spectroscopy data for these four PFCs were shown in Figure 1. The ^{19}F-based MR spectra of perfluorooctylbromide (PFOB) were shown in Figure 1a; the circled area marked by an arrow (44.8 ppm) denoted the selected magnetic resonance frequency for the excitation of PFOB. Perfluorodecalin (PFD) exhibited four distinct doublet peaks ([8.2, 7.7] ppm, [3.7, 3.2] ppm, [−2.9, −3.5] ppm, [−13.9, −14.4] ppm) as shown in Figure 1b (see Supporting Information, Figure S1); the doublet peak ([−13.9, −14.4] ppm) was chosen as the center frequency for the excitation of PFD. As seen in Figure 1c, the third PFC, 1,8-dichloroperfluorooctane (PFDOC), exhibited one singlet peak (58.2 ppm) and one triplet peak (6.3, 5.4, 4.8 ppm) (see Supporting Information, Figure S2); the singlet peak at 58.2 ppm was chosen as the excitation resonance frequency of PFDOC, to minimize the spectral overlap with the excitation center frequency of PFOB. For perfluoro-15-crown-5 ether (PFCE), the single peak at ∼36.3 ppm (see Supporting Information, Figure S3) was selected as the magnetic resonance frequency (Figure 1d). In the preliminary experimental results, distinct ^{19}F-based MR images were obtained using 600 MHz MR scanners (Figure 1), demonstrating the successful discrimination of the magnetic resonance frequencies of four different PFC materials. In a two-PFC mixture, MR images of PFOB and PFD were discriminated by the excitation of sample at magnetic resonance frequencies of 44.8 ppm and [−13.9, −14.4] ppm, respectively (Figure 1b). Introduction of PFDOC as a third component and excitation of the mixture at 58.2 ppm yielded a distinct ^{19}F-based MR image of PFDOC (Figure 1c). By exciting at ∼36.3 ppm, the MR image of PFCE could be distinguished from those of PFOB and PFDOC (Figure 1d). These results indicated that it was possible to obtain well-resolved signals from multiplexed MR images obtained in case

(10) Strijkers, G. J.; Mulder, W. J. M.; van Tilborg, G. A. F.; Nicolay, K. *Anticancer Agents Med. Chem.* **2007**, *7*, 291–305.
(11) Caravan, P. *Chem. Soc. Rev.* **2006**, *35*, 512–523.
(12) Bulte, J. W. M.; Kraitchman, D. L. *NMR Biomed.* **2004**, *17*, 484–499.
(13) Neuberger, T.; Schöpf, B.; Hofmann, H.; Hofmann, M.; Von Rechenberg, B. *J. Magn. Magn. Mater.* **2005**, *293*, 483–496.
(14) Lagerholm, B. C.; Wang, M.; Ernst, L. A.; Ly, D. H.; Liu, H.; Bruchez, M. P.; Waggoner, A. S. *Nano Lett.* **2004**, *4*, 2019–2022.
(15) Wu, C.; Hong, J.; Guo, X.; Huang, C.; Lai, J.; Zheng, J.; Chen, J.; Mu, X.; Zhao, Y. *Chem. Commun.* **2008**, 750–752.
(16) Geiss, G. K.; et al. *Nat. Biotechnol.* **2008**, *26*, 317–325.
(17) Li, Y.; Cu, Y. T. H.; Luo, D. *Nat. Biotechnol.* **2005**, *23*, 885–889.
(18) Prow, T. W.; Kotov, N. A.; Lvov, Y. M.; Rijnbrand, R.; Leary, J. F. *J. Mol. Histol.* **2004**, *35*, 555–564.
(19) Higuchi, M.; Iwata, N.; Matsuba, Y.; Sato, K.; Sasamoto, K.; Saido, T. C. *Nat. Neurosci.* **2005**, *8*, 527–533.
(20) Ahrens, E. T.; Flores, R.; Xu, H.; Morel, P. A. *Nat. Biotechnol.* **2005**, *23*, 983–987.
(21) Yu, J. X.; Kodibagkar, V. D.; Cui, W.; Mason, R. P. *Curr. Med. Chem.* **2005**, *12*, 819–848.
(22) Procissi, D.; Claus, F.; Burgman, P.; Koziorowski, J.; Chapman, J. D.; Thakur, S. B.; Matei, C.; Ling, C. C.; Koutcher, J. A. *Clin. Cancer Res.* **2007**, *13*, 3738–3747.
(23) Kim, S.; Lim, Y. T.; Soltesz, E. G.; De Grand, A. M.; Lee, J.; Nakayama, A.; Parker, J. A.; Mihaljevic, T.; Laurence, R. G.; Dor, D. M.; Cohn, L. H.; Bawendi, M. G.; Frangioni, J. V. *Nat. Biotechnol.* **2004**, *22*, 93–97.
(24) Gao, X.; Cui, Y.; Levenson, R. M.; Chung, L. W. K.; Nie, S. *Nat. Biotechnol.* **2004**, *22*, 969–976.
(25) Kim, S. W.; Zimmer, J. P.; Ohnishi, S.; Tracy, J. B.; Frangioni, J. V.; Bawendi, M. G. *J. Am. Chem. Soc.* **2005**, *127*, 10526–10532.
(26) Alivisatos, A. P.; Gu, W.; Larabell, C. *Ann. Rev. Biomed. Eng.* **2005**, *7*, 55–76.
(27) Medintz, I. L.; Uyeda, H. T.; Goldman, E. R.; Mattoussi, H. *Nat. Mater.* **2005**, *4*, 435–446.

Scheme 1. Schematic Illustration for the Preparation of Bimodal Imaging Nanoprobes Having Both ^{19}F-Based Multispectral Magnetic Resonance and Quantum Dots (QDs)-Based Multicolor Optical Imaging Capabilities[a]

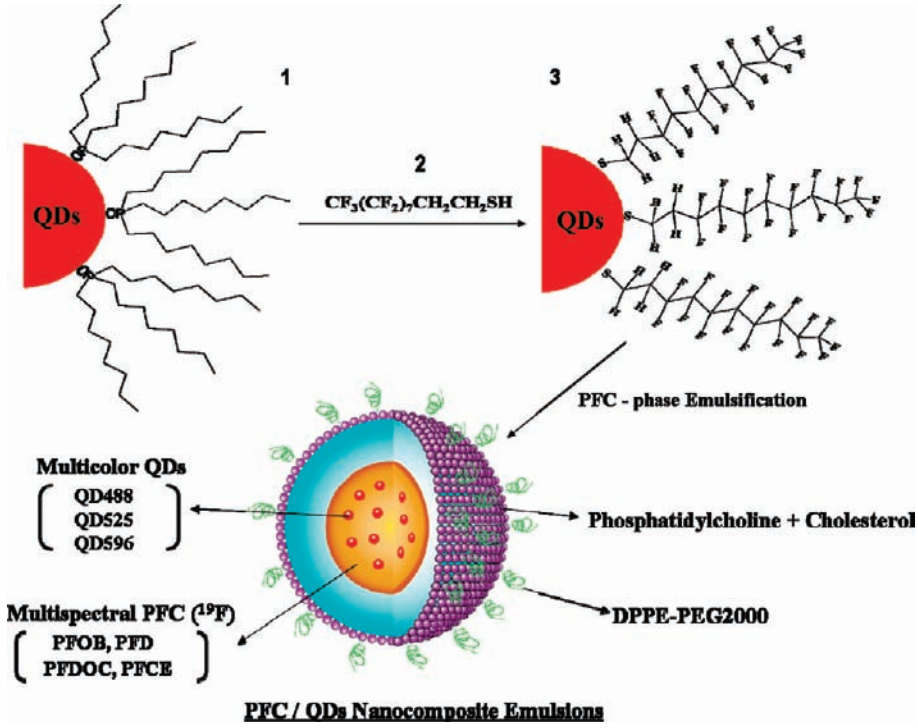

[a] Hydrophobic ligands of QDs (1) were exchanged with 1*H*,1*H*,2*H*,2*H*-perfluorooctanethiol (2). The dispersion of these QDs in perfluorocarbon (PFC) liquids was facilitated by the perfluorooctanethiol outer layers (3). Finally, QDs-containing PFC liquids were emulsified in aqueous solutions using various surfactants, such as phospholipids and cholesterols, to provide biocompatibility.

of combinations of different PFC materials each having a unique MR spectrum.

To incorporate optical imaging capabilities into the ^{19}F-based MR modality, we selected three different colored CdSe/ZnS QDs as optical imaging contrast agents. To combine the CdSe/ZnS QDs with PFC materials, QDs synthesized in organic solvents were moved into the PFC solution phase by ligand exchange. The phase movement of QDs in nonpolar organic solvents into the PFC phase could be achieved by virtue of the adsorption of fluorinated chemicals and displacement of the native hydrophobic ligand mixture (Scheme 1). The phase-movement process was conducted in a toluene−PFC mixture, in which the toluene phase contained a dispersion of CdSe/ZnS QDs capped with tri-*n*-octylphosphineoxide (TOPO), and the PFC liquid phase contained 1*H*,1*H*,2*H*,2*H*-perfluorooctanethiol ($CF_3(CF_2)_5(CH_2)_2SH$, PFOT). To induce contact between PFOT and the QDs, the toluene−PFC mixture was vigorously stirred until most of the QDs dispersed in the toluene phase partitioned into the PFC phase (see Experimental Section). The phase-movement results thus suggested that the TOPO ligands encapsulating CdSe/ZnS QDs were exchanged by PFOT, which induced the movement of QDs into the PFC phase (as seen from the inset in Figure 2a). X-ray photoelectron spectroscopy (XPS) measurement also showed the presence of 1*H*,1*H*,2*H*,2*H*-perfluorooctanethiol (distinct signal of the F[1s] electrons at 688.5 eV) on the surface of CdSe/ZnS QDs after ligand exchange reactions, while no traces of fluorine are shown in TOPO-coated CdSe/ZnS QDs (Figure S4). From the TEM images in Figure 2b, it was clearly observed that the CdSe/ZnS QDs were dispersed homogeneously in the PFD phase after the phase-movement phenomenon. Three-color emissions at different wavelengths, 488, 525, and 596 nm, were observed with excitation of the QDs using at a single wavelength of 352 nm (Figure 2c). The emission wavelengths of the three-colored CdSe/ZnS QDs were slightly blue-shifted after the QDs moved from the toluene phase to the PFD phase. The quantum yield (QY) of QDs dispersed in toluene was observed to be 51%, while PFOT-coated QDs dispersed in PFD solvent showed an increase to nearly 64%. Further, to investigate decay lifetime and carrier dynamics, time-resolved photoluminescence (TRPL) experiments were conducted at various laser excitation powers of 0.1, 0.5, and 1 mW, respectively. Figure 2d showed the decay curves obtained at varying excitation powers for QDs in toluene and PFOT-coated QDs in PFD, respectively. The decay curve for QDs in toluene displayed a nonexponential character, whereas PFOT-coated QDs in PFD tended to make the decay curve more exponential in behavior. The lifetime of the decreased intensities from maximum to 1/10 of its value (τ_{PL}) was used for simplicity. With increased excitation power of the laser, the estimated lifetime for PFOT-coated QDs dispersed in PFD (QDs in toluene) decreases from 52.3 ns (25.8 ns) for 0.1 mW to 46.8 ns (19.0 ns) for 1 mW. It was notable that the measured lifetimes for PFOT-coated QDs dispersed in PFD were longer than those for QDs in toluene in all of the excitation powers. This was indicative of a decrease in the probability of nonradiative recombination of carriers for PFOT-coated QDs in PFD resulting in better optical properties in comparison with QDs in toluene, as the lifetimes measured at room temperature were generally influenced by nonradiative recombination processes.[28,29]

For vital biological applications, it was necessary to transfer the PFC liquids containing CdSe/ZnS QDs into an aqueous

(28) Wuister, S. F.; Swart, I.; Van Driel, F.; Hickey, S. G.; De Mello Donegá, C. *Nano Lett.* **2003**, *3*, 503–507.
(29) Robin, I. C.; André, R.; Dang, L. S.; Mariette, H.; Tatarenko, S.; Gérard, J. M.; Kheng, K.; Tinjod, F.; Bartels, M.; Lischka, K.; Schikora, D. *Phys. Status Solidi B* **2004**, *241*, 542–545.

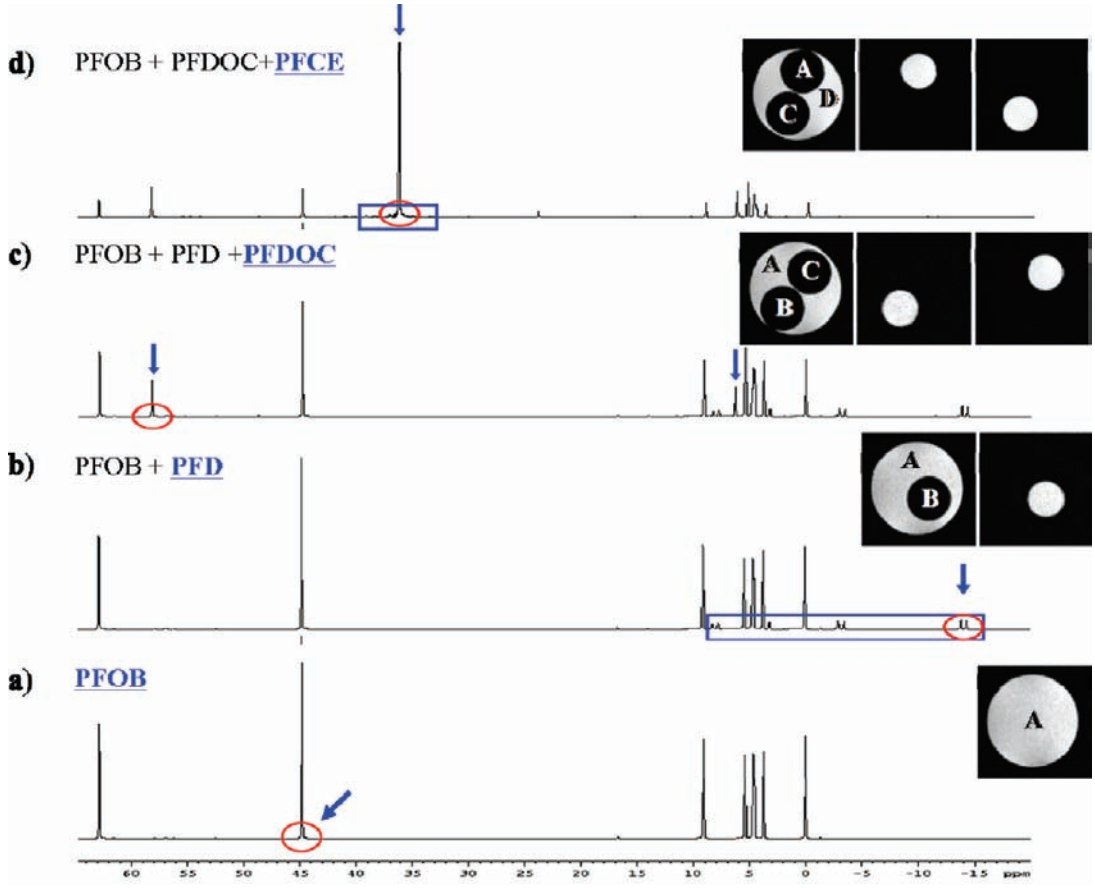

Figure 1. ^{19}F magnetic resonance spectra and images of (a) PFOB, (b) PFOB+PFD mixture, (c) PFOB+PFD+PFDOC mixture, and (d) PFOB+PFDOC+PFCE mixture, respectively. Resonance selective discrimination of ^{19}F MR image was obtained by excitation of the PFC or PFC mixtures at a resonance frequency corresponding to each PFC.

environment. The four different PFC liquids containing three different colored QDs were emulsified in aqueous solutions using various surfactants, including phospholipids and cholesterols (see Experimental Section). The average size and zeta potential of each PFC/[CdSe/ZnS QDs] nanocomposite emulsions, measured by light scattering analysis, were listed in Table S1. Figure 3a shows the cryo-TEM and TEM images of PFD/[CdSe/ZnS (596 nm) QDs] nanocomposites. Cryo-TEM image (inseted upper-left figure) showed that PFD/[CdSe/ZnS (596 nm) QDs] nanocomposite emulsions (250−290 nm size) were successfully fabricated by the emulsification process. Although some free liposomes or vesicles without PFD/QDs could be formed (Figure S5), most of the PFD/QDs liquids were encapsulated during the emulsification process. By controlling the concentration of lipid (surfactants) and the volume fraction of PFC liquids, the optimum experimental condition was achieved where the formation of free vesicular structures without PFC cores could be minimized. In the TEM images where the lipid layer was stained with phosphotungstic acid, CdSe/ZnS QDs (3−5 nm size) were observed in the PFD core phase. The emission curve of PFD/[CdSe/ZnS (596 nm) QDs] nanocomposite emulsions was indicated at a slightly red-shifted wavelength as compared to CdSe/ZnS QDs in toluene (Figure 3b).

To determine whether the PFC/QDs nanocomposite emulsions could be used for simultaneous detections using multispectral MR and multicolor optical imaging techniques, we prepared 12 spots corresponding to all of the permutations of the four different PFC liquids and three different color QDs ((1) of Figure 4a). The blue, green, and red emissions of QDs dispersed in the four different PFCs (PFOB, PFD, PFCE, PFDOC) were selectively captured using appropriate wavelength optical filters (see Experimental Section); each independent fluorescence signal was shown in (2)−(4) of Figure 4a. In each case, the desired emission was selectively acquired from the four different PFC/[CdSe/ZnS QDs] nanocomposite emulsions using the appropriate optical filter. Distinct ^{19}F-based MR signals ((5)−(8) of Figure 4a) were also acquired using the systematically tuned magnetic resonance frequencies for the excitation of each PFC/QDs nanocomposite emulsions (see Figure 1). The MR signals were discriminated solely on the basis PFC species (i.e., the resonance frequency) used in nanocomposite emulsions. In comparison with the conventional MR contrast agents (such as Gd-based or iron oxide nanoparticles), which used the magnetic relaxation properties of hydrogen (^{1}H), the above-mentioned engineered nanocomposite emulsions in current research offered the advantage of multiple detection capabilities using different PFCs with distinct MR-spectrum signatures. Our results indicated that any specific spot point in the 12-spot array shown in Figure 4a could be readily designated by simultaneous tuning of the optical filter and the magnetic resonance frequency. For example, the spot indicated by the white arrow in Figure 4a (1) could be easily selected using a green optical filter and the magnetic resonance frequency of PFCE. To assess the correlation between ^{19}F-based MR signal and fluorescence intensity, a calibration curve was obtained from serial dilutions of PFD/[CdSe/ZnS (596 nm) QDs] nanocomposites. ^{19}F signal was estimated using the area under the doublet peak ([−13.9, −14.4] ppm) in the ^{19}F-based NMR spectrum of PFD measured by a

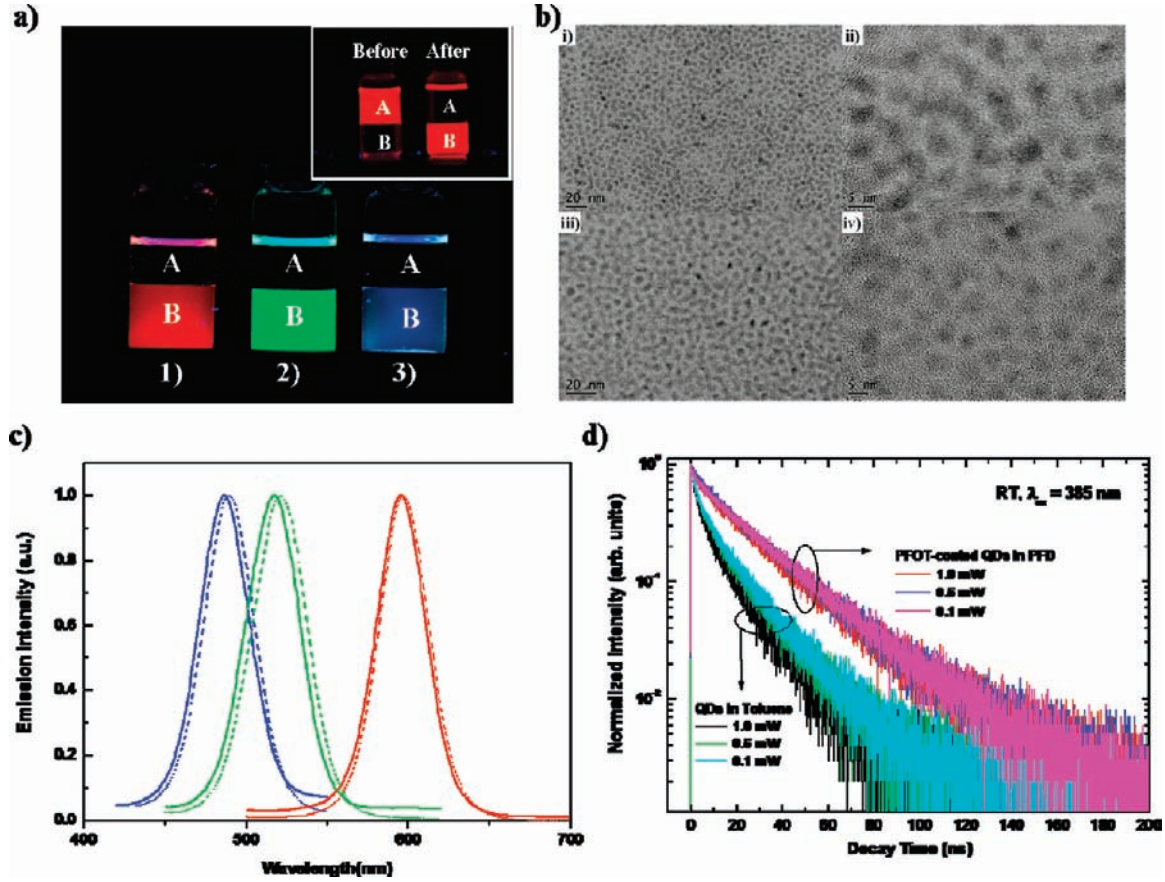

Figure 2. (a) Phase movement of three different colored CdSe/ZnS QDs in the toluene phase (A) into the PFD phase (B) [(1) 596 nm, (2) 525 nm, (3) 488 nm]. (b) TEM images of CdSe/ZnS QDs dispersed in toluene (1, 2) and PFD (3, 4). (c) Emission curve of three colored CdSe/ZnS QDs (488, 525, and 596 nm) dispersed in toluene (dotted line) and PFD (solid line). (d) Luminescence decay curves obtained at room temperature for CdSe/ZnS QDs dispersed in toluene and in PFD by using a pulsed Ti sapphire laser operating at an excitation wavelength of 385 nm.

600 MHz NMR spectrometer. Fluorescence intensity was also obtained from area under emission curve (excitation wavelength, 400 nm; emission wavelength, 455−655 nm). The plot of ^{19}F-based MR signals intensity versus fluorescence intensity indicated a linear correlation with $r^2 = 0.99501$ (Figure 4b). Using the linearity between ^{19}F-based MR signals and fluorescence, we could use the fluorescence detection method to quantify the PFC/QDs nanocomposite emulsions of ^{19}F-based MR imaging nanoprobes.

We have also investigated whether the multiple-detection capabilities of PFC/QDs nanocomposite emulsions could be applied to in vivo conditions. There has been a strong interest in developing and validating imaging technologies that can visualize cell-based therapies involving T cells, dendritic cells, and macrophages.[30,31] Multiple detection imaging techniques of these labeled immune cells will provide a capacity to detect interactions between immune cells, and help to unravel the complex biological mechanisms that underlie immune cell-based therapies. As a model study, three different nanocomposite emulsions samples, PFDOC/[CdSe/ZnS (525 nm) QDs], PFDOC/[CdSe/ZnS (596 nm) QDs], and PFOB/[CdSe/ZnS (596 nm) QDs], were prepared and used for labeling of three different immune cells (macrophage cells, T cells, and dendritic cells). The uptake of nanocomposite emulsions by phagocytic cells such as macrophages and dendritic cells was concentration dependent. The efficiency of intracellular delivery was up to 90.55% in macrophages and 85.34% in dendritic cells (Figure 5). These imaging probes also served as a novel platform nanotechnology for easily and efficiently labeling of T cells, which are normally resistant to the transfer of exogenous contrast (Figure 5). As compared to that of the phagocytic cells, the nanocomposite emulsions uptake efficiency of T cells was up to 33%. The viability of immune cells after labeling with PFC/QDs nanocomposite emulsions was negligible, when the concentration of nanocomposite emulsions was up to 25 mg/mL (Figure S6). We have also investigated the effect of PFC/QDs nanocomposite emulsion on cell phenotype and cell function. As an example, we examined the effect of labeling on the dendritic cells maturation and migration function. We have observed that the labeling of cells with PFC/QDs nanocomposite emulsions has little effect on the dendritic cells maturation and migration in the concentration range that was used for cell imaging (up to the concentration of 25 mg/mL) (Figure S7). The cellular image that represents the intracellular localization of PFC/QDs nanocomposite emulsions within the cells showed that most of them reside in the lysosome (Figure S8). The stability of fabricated PFC/QDs nanocomposite emulsions was also examined at various conditions. To investigate long-time stability of nanocomposite emulsions, they were stored at 4 and 37 °C for 2 months (Figure S9). The particle diameter was measured by DLS measurements. There was no significant variation in average diameter. For serum stability test, the

(30) Akins, E. J.; Dubey, P. *J. Nucl. Med.* **2008**, *49*, 180S–195S.
(31) Lucignani, G.; Ottobrini, L.; Martelli, C.; Rescigno, M.; Clerici, M. *Trends Biotechnol.* **2006**, *24*, 410–418.

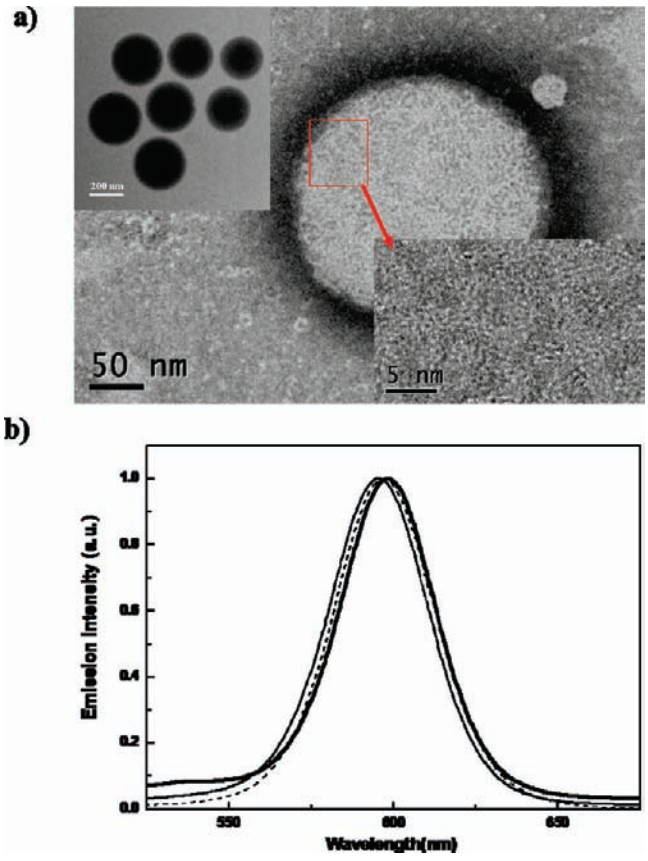

Figure 3. (a) TEM and cryo-TEM images and (b) emission curve of PFD/[CdSe/ZnS (596 nm) QDs] nanocomposite emulsions. Each line represents CdSe/ZnS (596 nm) QDs in toluene (dashed line), CdSe/ZnS (596 nm) QDs in PFD (thin solid line), and PFD/[CdSe/ZnS (596 nm) QDs] nanocomposite emulsions (thick solid line), respectively.

nanocomposite emulsions were treated with 10% (v/v) FBS in RPMI at 37 °C for 24 h. No significant change in diameter was observed, which means they were stable in serum condition.

Based on in vitro experimental data, the labeled immune cells were subcutaneously injected into the different body parts of a mouse (Figure 6a). Immune cells labeled with bimodal imaging contrast agents may provide an exact detection and localization of the labeled cells in vivo condition through MR and optical imaging. Using an optical filter (525WB20), green fluorescence signals were selectively detected at point A, where macrophage cells labeled with PFDOC/[CdSe/ZnS (525 nm) QDs] were injected (Figure 6b). After changing the optical filter with red filter (600WB20), red fluorescence signals were also detected at points B and C, where T cells labeled with PFDOC/[CdSe/ZnS (596 nm) QDs] and dendritic cells labeled with PFOB/[CdSe/ZnS (596 nm) QDs]) were injected, respectively (Figure 6c).

Both ^{1}H-based (Figure 6d) and ^{19}F-based MR images (Figure 6e,f) were obtained. When the magnetic excitation resonance frequency was matched with that of PFDOC, selective MR images were generated at points A and B where the macrophage cells labeled with PFDOC/[CdSe/ZnS (525 nm) QDs] and T cells labeled with PFDOC/[CdSe/ZnS (596 nm) QDs]) were injected, respectively (Figure 6e). Distinct MR image was also observed at point C where the dendritic cells labeled with PFOB/[CdSe/ZnS (596 nm) QDs] were injected (Figure 6f), with the matched resonance frequency of PFOB. While the ^{1}H-based MR image provides a whole body image, the ^{19}F-based MR image shows the only signals generated from the injected immune cells labeled with PFC/QDs nanocomposite emulsions. In case of the ^{19}F-based MR image, there was no background signal, which is one of the distinctive advantages of ^{19}F-based MRI technique as compared to the ^{1}H-based MRI. The in vivo fluorescence and MR image analysis showed that signal intensities from macrophages and dendritic cells were 2.5−3 times higher than that of T cells (Figures S10, S11). The low signal intensity of T cells can be related to the low efficiency in the uptake of PFC/QDs nanocomposite emulsions as shown in Figure 5. Furthermore, the minimum concentration of labeled cells needed to be detected at a given location is also dependent on the cell type because the uptake of PFC/QDs nanocomposite emulsions was different according to cell type. The uptake efficiency was high in macrophages and dendritic cells, while it was low in T cells. We have examined the sensitivity of our detection system. To investigate the sensitivity of detection system, serially diluted dendritic cells labeled with PFOB/[CdSe/ZnS (596 nm) QDs)] nanocomposite emulsions were subcutaneously injected, and the signal was detected. As shown in Figure S12, we could get the ^{19}F MR signals when the concentration of labeled dendritic cells was up to 5×10^{6} cells, whereas the optical fluorescence signal was still detected when the concentration was lowered up to 2×10^{6} cells. Using the correlation between ^{19}F-based MR signals (or fluorescence intensity) and the number of cells, we could approximately quantify the number of cells at a given location. As for optical imaging, the sensitivity of detection system is dependent on the camera sensitivity, various optical parameters of target tissues (such as light absorption and scattering properties of tissues), emission wavelength of optical probes, and tissue depth, etc.[23] In case of ^{19}F MR imaging, the signal detection of labeled cells at a given location is highly dependent on the tesla of the MR equipment and the used RF coils, which are the antenna of the MRI system that excites the MR signal within the mouse and/or receives the return signal.[21] Therefore, the MR detection equipment and optical imaging system should be optimized for sensitive signal detection.

With regards to in vivo toxicity, most fluorocarbons are known to be innocuous and physiologically inactive: in fact, no toxicity, carcinogenicity, or mutagenic effects have been reported for perfluorocarbons.[32] However, the systematic study on the final fate of the perfluorocarbons used for cell labeling in vivo conditions should be conducted in future research. Taken together, the engineered PFC/QDs nanocomposite emulsions were presented as the first platform materials that render simultaneous multispectral MR and multicolor fluorescence detection to be feasible both in vitro and in vivo, by the incorporation of the multicolor emission properties of QDs with fluorine (^{19}F)-based multispectral MR imaging properties of PFCs (Figures 5 and 6).

The experimental data showed that the novel-type of bimodal imaging contrast agents revealed in this study could be used for multiplexed molecular imaging of immunotherapeutic cells. As compared to the other bimodal imaging nanoprobes based on ^{1}H-based MR contrast agents (gadolinium or iron oxide nanoparticles) and QDs, the PFC/QDs nanocomposite emulsions are capable of distinguishing multiple targets simultaneously through both multispectral ^{19}F-based MR and multicolor fluorescence imaging mode. Most of all, the multispectral capability of PFC/QDs nanocomposite emulsions containing spectrally distinct PFCs could be used to be simultaneously targeted and independently imaged. The multispectral properties of PFCs

(32) Longstaff, E. *Ann. N.Y. Acad. Sci.* **1988**, *534*, 283–298.

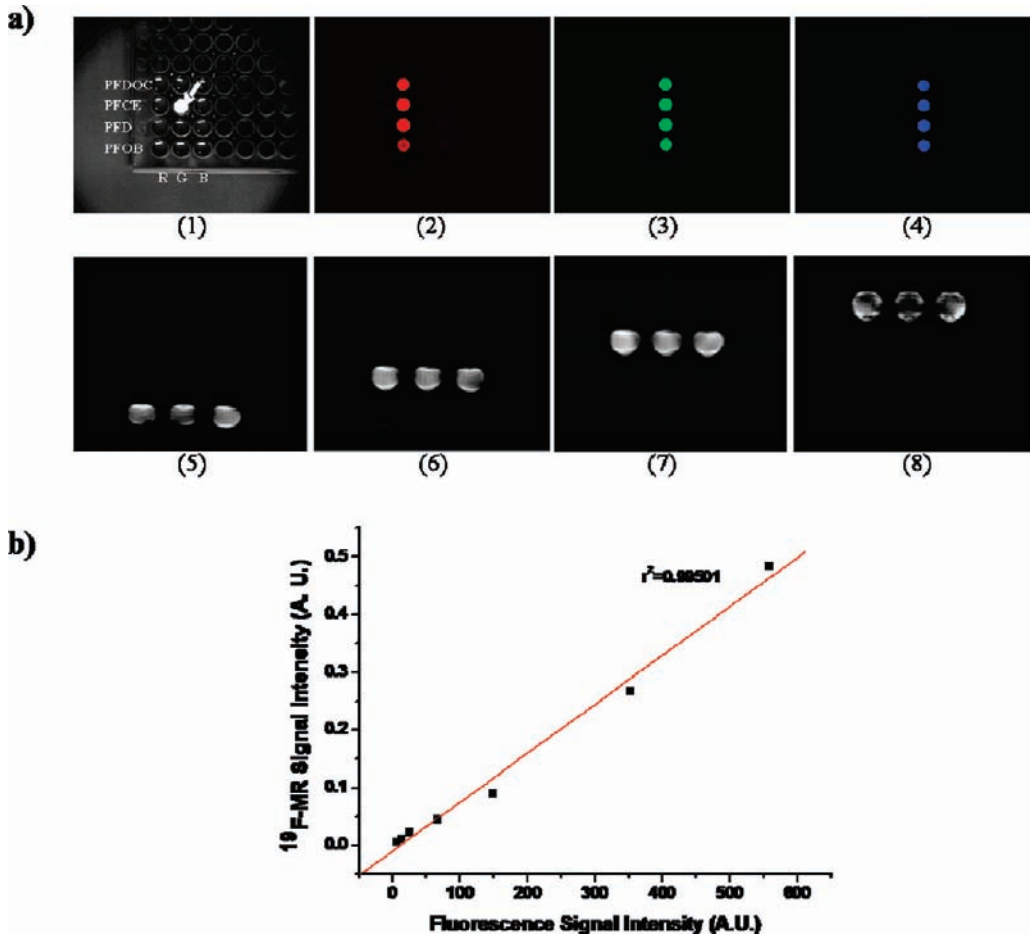

Figure 4. (a) Multicolor fluorescence [(2)−(4)] and resonance selective ^{19}F MR [(5)−(8)] detection of PFC/[CdSe/ZnS QDs] nanocomposite emulsions: (1) color image, (2) image obtained by using a red filter, (3) image obtained by using a green filter, (4) image obtained by using a blue filter, (5) PFOB-resonance selective MR image, (6) PFD-resonance selective MR image, (7) PFCE-resonance selective MR image, and (8) PFDOC-resonance selective MR image. (b) Calibration curve representing the correlation between ^{19}F-based MR signals and fluorescence intensity.

could be extended by mixing different concentrations of each PFC and deconvolution of their spectral signal. Although ^{19}F-based MR has excellent properties for MR detection and imaging in the sense that the background concentration of fluorine is essentially undetectable, the fluorine signal is intrinsically weak as compared to that of protons in view of the limited concentration. Previous studies have reported the minimum detectable limit of ^{19}F at 1.5 T is 30 μM.[33] Although this concentration would be difficult to achieve with a circulating agent that might passively accumulate at a selected site in vivo, the PFC/QD nanocomposite emulsions can overcome the limitation because the internalization permits local accumulation of nanocomposite emulsions within cells and each individual nanocomposite emulsion carries an extremely high payload of fluorine (~100 M).[33] Therefore, we expect that the PFC/QDs nanocomposite emulsions could be used as molecular imaging probes for cell-based therapy. Another disadvantage of the present PFC/QDs nanocomposite emulsions is the use of CdSe/ZnS QDs, of which potential toxicity of CdSe/ZnS QDs to live cells has been reported.[34] In this sense, the development of new QDs based on noncadmium metal would be a very promising future research topic. However, the photostability of PFC/QDs nanocomposite emulsions was excellent as compared to that of existing conventional fluorescent dyes (CFSE). When the 488 nm wavelength light was illuminated on cells, the fluorescence signal from dendritic cells labeled with CFSE organic dye started to decrease only after 10 s, while that from dendritic cells labeled with PFC/QDs nanocomposite emulsions was still high even after 20 min (Figure S13). Although the emission wavelength (525, 596 nm) of QDs used in this study was not bad to get in vivo images through thin tissues, such as hairless mouse skin (about 210 μm), it needs QDs emitting in the longer wavelength region for us to get imaging signal even in the deep tissues. If we consider light transmission through biological tissue increases at longer wavelength regions of the spectrum, near-infrared or infrared emitting QDs could be used for future optical-based in vivo imaging applications in more deeper tissues.[23,25]

The dilution of PFC/QD nanocomposite emulsions with division of cells would be another critical factor to consider in clinical applications because the signal would be also decreased with the cell division. The retention of nanocomposite emulsions within cells was investigated by fluorescence microscopy. The fluorescence intensity of nanocomposite emulsions decreased with the division of labeled cells. In case of cell lines such as macrophage cell lines (RAW264.7) and dendritic cell lines (DC2.4), the fluorescence intensity was decreased up to 30%

(33) Lanza, G. M.; Winter, P. M.; Neubauer, A. M.; Caruthers, S. D.; Hockett, F. D.; Wickline, S. A. *Curr. Top. Dev. Biol.* **2005**, *70*, 57–76.
(34) Chang, E.; Thekkek, N.; Yu, W. W.; Colvin, V. L.; Drezek, R. *Small* **2006**, *2*, 1412–1417.

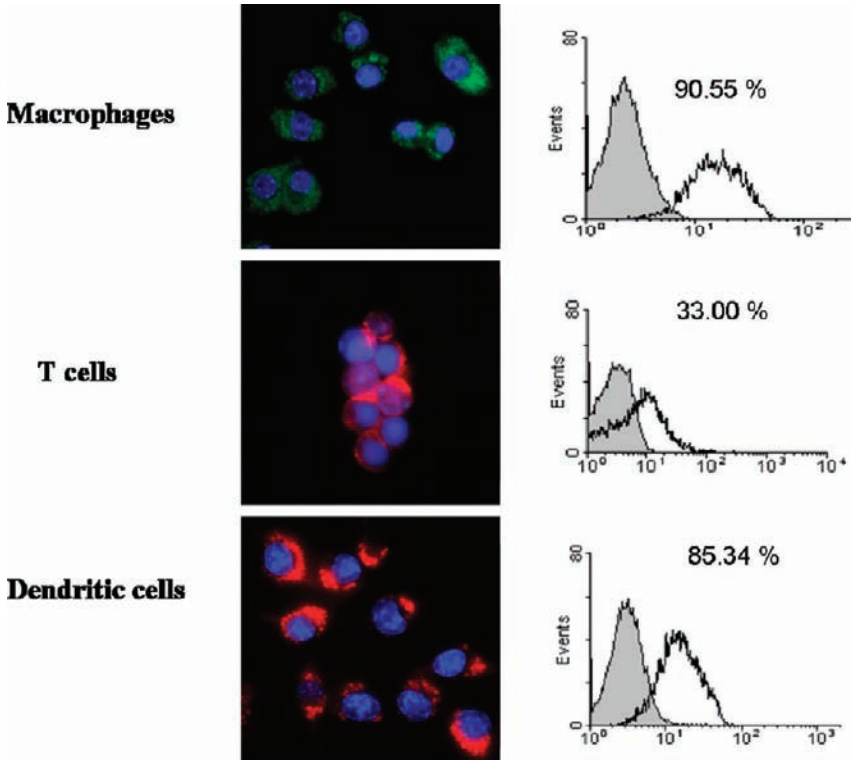

Figure 5. Fluorescence microscopic images and flow cytometry analysis of immunotherapeutic cells labeled with PFC/[CdSe/ZnS QDs] nanocomposite emulsions (10 mg/mL). Macrophage and T cells were labeled with PFDOC/[CdSe/ZnS (525 nm) QDs] and PFDOC/[CdSe/ZnS (596 nm) QDs], respectively. Dendritic cells were labeled with PFOB/[CdSe/ZnS (596 nm) QDs]. The % number represents positive percentage of labeled cells.

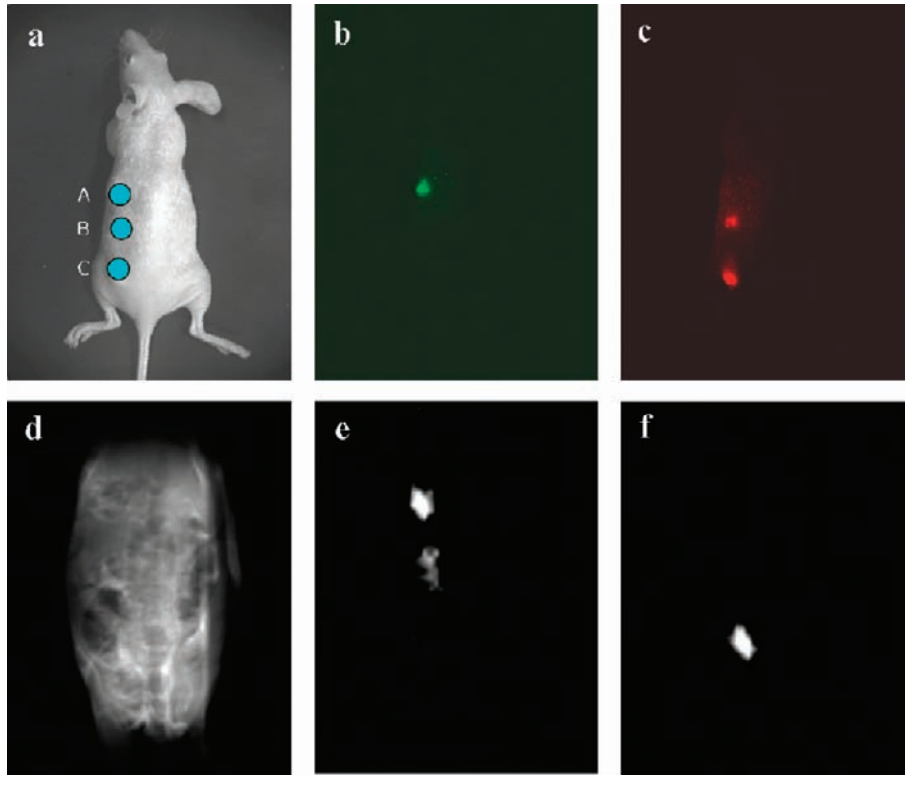

Figure 6. In vivo detection. (a) Black and white image of the mouse injected with three different types of immune cells (5×10^6 to 1×10^7 cells/mL) labeled with PFC/[CdSe/ZnS QDs] nanocomposite emulsions: (A) Macrophage cells labeled with PFDOC/[CdSe/ZnS (525 nm) QDs]; (B) T cells labeled with PFDOC/[CdSe/ZnS (596 nm) QDs]; and (C) dendritic cells labeled with PFOB/[CdSe/ZnS (596 nm) QDs]; (b) image obtained by using a green filter (525WB20); (c) image obtained by using a red filter (600WB20); (d) ^{1}H MR image; (e) PFDOC-resonance selective MR image; and (f) PFOB-resonance selective MR image.

of initial value after 2 days. In contrast, the decrease of fluorescence intensities in BM-DCs (bone marrow derived dendritic cells) and T cells, which were directly acquired from mouse, was smaller than that in cell lines (Figure S14).

Furthermore, the PFC/QD nanocomposite emulsions can be also used as multifunctional drug delivery vehicles by integrating five functions into one delivery vehicle utilizing a therapeutic drug, tumor targeting, an imaging agent, a pO_2 probe, and an O_2 carrier.[35]

Conclusion

In summary, we described the fabrication of PFC/QDs nanocomposite emulsions as a novel type of multimodal imaging nanoprobe, by incorporating the ^{19}F-based multispectral MR properties of PFC materials into the multicolored emission properties of QDs. The multispectral MR capability of PFC/QDs nanocomposite emulsions was shown by selective excitation of the nanocomposite emulsions with magnetic resonance frequency of each PFC, while the multicolor detection performance of them could be achieved using appropriate wavelength selection. Finally, PFC/QDs nanocomposite emulsions were successfully applied to differentially visualize immunotherapeutic cells in vivo through multispectral MR and multicolor optical imaging. The multispectral properties of PFC/QDs nanocomposite emulsions could be extended by mixing different concentrations of each PFC having distinct resonance frequency, while the optical multiplexing of QDs could also be extended by multiplexing wavelengths and their intensities. Taken together, the novel concepts and materials presented in this research could open new opportunities for multiplex detections with applications in medical diagnostics (e.g., detection of multiple analytes), and multiple labeling of different cells or organelles both in vitro and in vivo.

Experimental Section

Preparation of PFC/QDs Nanocomposites. To fabricate PFC/QDs nanocomposites, four PFC materials [perfluorodecalin (PFD, SynQuest Laboratories, Alachua, FL), perfluoro-15-crown-5 ether (PFCE, SynQuest Laboratories, Alachua, FL), perfluorodioctylchloride (PFDOC, SynQuest Laboratories, Alachua, FL), perfluorooctylbromide (PFOB, Aldrich, St. Louis, MO)] and three different colored QDs (emitting at 488, 525, 596 nm, Evident Technologies, Troy, NY) were used. For ligand-exchange, 4 mL of CdSe/ZnS QDs dispersed in toluene (2.5 mg/mL) was washed three times with methanol and mixed with PFC liquids (4 mL) containing 50 μL of 1*H*,1*H*,2*H*,2*H*-perfluorooctanethiol (Fluorochem, Derbyshire, UK). After vigorous mixing of the two-phase solution at nitrogen atmosphere for 36 h at room temperature (or 6−24 h at 60 °C), the CdSe/ZnS QDs were partitioned into the PFC phase. The CdSe/ZnS QDs in PFC liquids were then washed three times with methanol. Next, PFC liquids containing CdSe/ZnS QDs were emulsified in an aqueous solution using surfactant mixtures. A surfactant mixture comprising of 64 mol % lecithin (L-α-phosphatidylcholine 95%, chicken egg, Avanti Polar Lipids, Alabaster, AL), 35 mol % cholesterol (Avanti Polar Lipids, Alabaster, AL), and 1 mol % 1,2-dipalmitoyl-*sn*-glycero-3-phosphoethanolamine-*N*-[methoxy(polyethylene glycol)-2000] (ammonium salt) (mPEG2000-PE, Avanti Polar Lipids, Alabaster, AL) was dissolved in chloroform, and the organic solvent was evaporated using a rotary evaporator and a vacuum oven (50 °C) for 24 h. After the surfactant mixture was dispersed into sterilized distilled water, the solution was sonicated. PFC liquids (40% v/v) containing CdSe/ZnS QDs (1.7% w/v), glycerin (2.0% w/v), surfactant mixture, and distilled water were mixed for 30 s using a homogenizer. The mixture was processed through an emulsifier (M-110S, Microfluidics, Newton, MA) at 20 000 psi for 4 min. The fabricated PFC/[CdSe/ZnS QDs] nanocomposites were stored at 4 °C.

Characterization. The absorption and emission spectra of CdSe/ZnS QDs in toluene, PFC, and PFC/[CdSe/ZnS QDs] nanocomposites were measured using a fluorescence spectrometer (LS 55, PerkinElmer Instruments, Wellesley, MA). Photoluminescence quantum yields (QY) were obtained by comparing the QD samples with a standard reference dye (Rhodamine 6G in water) and by using the data derived from the luminescence and the absorption spectra.

$$\mathrm{QY} = \left(\frac{1 - T_{\mathrm{ST}}}{1 - T_{\mathrm{X}}}\right)\left(\frac{\Delta\Phi_{\mathrm{X}}}{\Delta\Phi_{\mathrm{ST}}}\right)q_{\mathrm{ST}}$$

where T_{ST} and T_X are the transmittances at 488 nm for the standard reference and the QDs samples, respectively. $\Delta\Phi_{ST}$ and $\Delta\Phi_X$ gave the integrated emitted photon flux for the reference sample and the QDs sample, respectively. q_{ST} represents the quantum yield of the standard sample. To obtain quantum yield of the QDs dispersed in different solvents, UV−vis absorption and fluorescence spectra were measured. UV−vis absorption spectra were recorded on a Jenway (Genova, Dunmow, UK) spectrophotometer. Diluted solutions of the QDs were placed in a 1 cm quartz cuvette, and their absorption and corresponding fluorescence spectra were measured. The photoluminescence spectra were recorded on a spectrometer (Acton 2300i, Acton, MA). The room-temperature quantum yields were determined by comparing these samples with a standard reference organic dye, Rhodamine 6G, in water with a quantum yield of 95%. For the time-resolved photoluminescence (TRPL) experiments, a pulsed laser beam produced by a Ti:sapphire mode-locked and cavity dumped laser was frequency-doubled using a β-barium borate (BBO) nonlinear optical crystal and was used as an excitation source of light. The excitation wavelength was 385 nm. The fluorescence decay signals from the sample were detected by a microchannel plate photomultiplier tube (MCP-PMT, Hamamatsu, R3809U-51), and the time-correlated signal was analyzed by a time-correlated single-photon counting system (TCSPC, PicoQuant, PicoHarp 300, Berlin, Germany). The measured fluorescence decay values were estimated by the deconvolution process with an instrument response function (IRF) of about 45 ps. The process of ligand exchange was studied by X-ray photoelectron spectroscopy (XPS). The samples were prepared on indium−tin−oxide coated glass and transferred into a vacuum chamber for XPS measurements. The XPS spectra were measured using Mg Kα radiation ($\hbar\omega$ = 1253.6 eV) and a SES-100 analyzer (Gamadata) equipped with a 2D CCD detector. Those give the total energy resolutions of 1.4 and 0.9 eV for survey and each core level spectrum, respectively. The mean particle diameters and zeta (ζ)-potentials of the PFC/[CdSe/ZnS QDs] nanocomposites were determined using a particle size analyzer (ELS-Z, Otsuka Electronics, Japan). The intensity autocorrelations were measured at a scattering angle (θ) of 90° with electrophoretic light scattering at 25 ± 0.1 °C. TEM images were obtained using a 200 kV field emission transmission electron microscope (JEM-2100F, JEOL, Ltd., Tokyo, Japan). The samples were stained with 1% phosphotungstic acid and placed on copper grids with Formvart films. PFC/[CdSe/ZnS QDs] nanocomposites were also prepared as a thin liquid layer supported on a cryo-grid and were immediately plunged in liquid ethane to prevent evaporation from the thinly spread sample. The frozen grids were stored in liquid nitrogen and transferred in a GATAN model 630 cryotransfer (Gatan, Inc., Warrendale, PA) in liquid nitrogen at a temperature of approximately −185 °C. Direct imaging was carried out using an acceleration voltage of 120 kV and a Multiscan 600W charge-coupled device (CCD) camera (Gatan, Inc., Pleasanton, CA) at a temperature of approximately −170 °C.

Fluorescence Imaging and ^{19}F MR Spectroscopy and Imaging of Nanocomposites. Fluorescence images of PFC/[CdSe/ZnS QDs] nanocomposites were obtained using an imaging system consisting of an excitation light source and a cold CCD camera (Orca ERG; Hamamatsu Photonics, Bridgewater, NJ), designed and built in our laboratory. Twelve different PFC/QDs nanocomposites

(35) Yu, Y. B. *J. Drug Targeting* **2006**, *14*, 663–669.

(200 μL volumes), corresponding to all permutations of the four different PFC liquids and three different colored QDs, were placed in a well plate (4 columns × 3 rows). The blue, green, and red emissions of QDs dispersed in the four different PFCs were selectively captured using the appropriate emission filters (480WB20, 525WB20, 600WB20, Omega Optical, Brattleboro, VT). All images were processed by using Simple PCI software (Compix Inc., Lake Oswego, OR). All ^{19}F spectral and imaging experiments of PFC liquids were performed on a 600 MHz (14 T) Bruker NMR spectrometer (Avance DMX600, Bruker, Rheinstetten, Germany) equipped with a triple gradient system for microscopic imaging. The maximum gradient strength was 200 G/cm, and a 5 mm double-tuned ^{1}H/^{19}F saddle-type RF coil was used. For ^{19}F spectral measurement of PFC liquids, four different PFC liquids (PFOB, PFD, PFDOC, and PFCE) were inserted into standard Wilmad 5 mm NMR tubes, and fluorine spectra (30° flip angle; 2 acquisitions; 5 s acquisition time) were acquired from each sample. Four PFC liquids were imaged with a gradient echo sequence (64 × 64 matrix; 5 × 5 mm^2 FOV; 100.0 ms TR; 2.4 ms TE; 5 mm slice thickness; 2 acquisitions; 6 s acquisition time; 60° flip angle) using the chemical shift selective method. To differentiate each fluorine-base MR image, we have designed a special geometry for sample filling: two 1.9 mm (inner diameter = 1.5 mm) capillary tubes were inserted into standard Wilmad 5 mm NMR tubes. In a control experiment, one NMR tube was filled with PFOB, while another capillary tube was filled with PFD and a third capillary tube was filled with PFDOC. The distinct fluorine-based MR image of specific PFC from PFC mixture was collected by exciting the PFC mixture at the resonance peak of each PFC liquid (chemical shift selective method). PFC/QDs nanocomposites were imaged with a 4.7 T Bruker scanner (BioSpec, Rheinstetten, Germany) using a double-tuned ^{1}H/^{19}F Birdcage coil design (outer/inner: 59/35 mm). To acquire fluorine MR images, 12 different PFC/QDs nanocomposites were placed in a well plate (4 columns × 3 rows). The volume of emulsion contained in each well plate was about 200 μL. They were imaged with a gradient echo sequence (128 × 128 matrix; 50 × 50 mm^2 FOV; 50.0 ms TR; 6 ms TE; 5 mm slice thickness; 16 acquisitions; 1.42 s acquisition time; 60° flip angle). Distinct fluorine MR images of PFC/QDs nanocomposites were achieved by exciting samples at the resonance frequency corresponding to each PFC (obtained from the above fluorine spectral experiments). Other peaks neighboring to the main resonance peak were suppressed by the frequency selective saturation method.

In Vitro and In Vivo Fluorescence and ^{19}F MR Imaging of Immune Cells. RAW264.7 (murine macrophage cells; ATCC) and DC2.4 cells (murine dendritic cells) were cultured in 10 mm dishes (1 × 10^7/dish) in Dulbecco's modified Eagle Medium (DMEM; Gibco, Invitrogen, Carlsbad, CA) supplemented with 10% heat in activated FBS, 50 IU/mL penicillin, and 50 μg/mL streptomycin. Bone marrow-derived dendritic cells (BM-DCs) were induced to differentiate in vitro using a method previously described. Briefly, 2 × 10^6 BM cells were cultured for 7−8 days with 20 ng/mL mouse recombinant granulocyte-macrophage colony-stimulating factor (GM-CSF; R&D Systems, MN). T cells were obtained from splenic mononuclear cells of normal BALB/c mice using a MACS mouse pan T cell isolation kit (Miltenyi Biotec Inc., Auburn, CA). The purified T cells were cultured with 100 U/mL IL-2 in 96 well plates (3 × 10^6/mL). For fluorescence imaging, RAW264.7, DC2.4, BM-DCs, or T cells were incubated with 50 μL/mL nanocomposites (PFDOC/[CdSe/ZnS (525 nm) QDs], PFOB/[CdSe/ZnS (596 nm) QDs], PFDOC/[CdSe/ZnS (596 nm) QDs]) for 24 h at 37 °C. After being washed with PBS, the labeled cells were fixed with Cytofix/Cytoperm solution and stained with DAPI in PBS. Fluorescence images were obtained on a Deltavision RT deconvolution microscope (Applied Precision Technologies, Issaquah, WA) using emission filters (525WB20, 600WB20, Omega Optical, Brattleboro, VT). To detect intracellular localization of nanocomposite emulsions to lysosomes, RAW264.7 cells were stained with the lysosomal marker lysosome-associated membrane glycoprotein-1 (LAMP-1) by incubating with PE-conjugated rat anti-LAMP-1 monoclonal antibody (1D4B) (eBioscience, San Diego, CA) for 30 min at room temperature, and fluorescence images were obtained as described above. Cell viability was assessed using an Annexin-V-FLUOS Staining Kit (Roche Applied Science, Penzberg, Germany). Briefly, cells were incubated with 50 μL/mL nanocomposite emulsions for 24 h. Also, the cells were stained with annexin V-FITC for 15 min at room temperature in the dark. The stained cells were analyzed by FACScalibur (Becton Dickinson, Mountain View, CA). The percent survival rate represents the Annexin V-negative cell population. To detect intracellular retention of nanocomposite emulsions over time in cultured immune cells, DC2.4, BM-DCs, RAW264.7, or T cells were initially labeled for 24 h (day 0), washed three times, and reincubated for 3 days. The retention rate was analyzed by using flow cytometry.

For in vivo fluorescence and MR imaging, RAW264.7, BM-DCs, DC2.4, and T cells (5 × 10^6 to 1 × 10^7 cells/mL) labeled with a nanocomposite emulsions were resuspended in 100 μL of HBSS buffer and were subcutaneously injected into the different body parts of a mouse. The mice were anesthetized with 300 μL of a 2.5% avertin solution (2,2,2-tribromoethanol-*tert*-amyl alcohol, Sigma). Thereafter, fluorescence images (1−20 s exposure) were obtained using an excitation light source (425 nm) and an emission filter (525WB20 or 600WB20). All images were processed with Simple PCI software (Compix Inc., Cranberry Township, PA). ^{19}F MR images of the mouse were performed with 4.7 T Bruker scanner (BioSpec, Rheinstetten, Germany) using a double-tuned ^{1}H/^{19}F Birdcage coil design (outer/inner: 59/35 mm). For the ^{19}F MR image, the mouse was imaged with a gradient echo sequence (128 × 128 matrix; 60 × 60 mm^2 FOV; 50.0 ms TR; 2 ms TE; 5 mm slice thickness; 20 acquisitions). The distinct fluorine MR images of the mouse were acquired by exciting the samples at the resonance frequencies of PFOB and PFDOC, respectively. Other neighboring peaks from the resonance peak were suppressed by the selective frequency saturation method.

Acknowledgment. We acknowledge the financial support received from the Pioneer Research Center Program (Grant No. 2008-00180, MEST, Korea), the National Research Foundation (NRF), and the KRIBB Research Initiative Program. We are also thankful to Dr. Jeong Won Kim in KRISS for the measurement of XPS.

Supporting Information Available: Experimental data. Complete ref 16. This material is available free of charge via the Internet at http://pubs.acs.org.

JA904472Z